Room-temperature oxygen diffusion and ordering in $YBa_2Cu_3O_{7-y}$ studied with time-resolved Raman spectroscopy

I. Poberaj, D. Mihailović,* and S. Bernik
Jozef Stefan Institute and Faculty of Sciences, E. Kardelj Univeristy of Ljubljana, Jamova 39, 61111 Ljubljana, Yugoslavia
(Received 6 September 1989)

Oxygen diffusion and ordering is studied in $YBa_2Cu_3O_{7-\delta}$ single crystals as a function of time after oxygen is ejected from the surface with a strong laser pulse. Features in the Raman spectra that are sensitive to oxygen concentration and disorder are monitored by time-resolved spectroscopy. The experiments clearly show that room-temperature diffusion takes place from the bulk $YBa_2Cu_3O_7$ into the oxygen-depleted $YBa_2Cu_3O_{6+y}$ surface. There appear to be a fast ($\tau < 5$ ms) and a relatively slow ($\tau > 1$ min) lifetime to the observed features. We suggest that diffusion in $YBa_2Cu_3O_{6+y}$, which is shown to proceed via hopping of oxygen along vacancy positions, may be aided by anharmonic features of the lattice in addition to the chemical potential gradient at the $YBa_2Cu_3O_{6+y}$ (surface)–$YBa_2Cu_3O_7$ (bulk) interface.

Since the discovery[1] that oxygen concentration plays a major role in doping of the $YBa_2Cu_3O_{7-\delta}$ system and the associated superconducting-metal-insulator transition, as well as determining whether the structure is orthorhombic or tetragonal, a number of authors have studied the effects of oxygen ordering[2] as well as transport and diffusion of oxygen at high temperatures.[3,4] In this communication we report room temperature measurements of surface oxygen concentration δ and vacancy ordering in $YBa_2Cu_3O_{7-\delta}$ single crystals by means of Raman spectroscopy. Time resolved measurements are performed by first illuminating the sample with a strong laser pulse and the changes in the Raman spectrum are then monitored as a function of time with delayed weak laser pulses.

Raman spectra of $YBa_2Cu_3O_{7-\delta}$ for different oxygen concentrations have been studied in detail by a number of authors.[5,6] For an extensive review of the Raman investigations of superconducting high-T_c oxides the reader is referred to a paper by Thomsen and Cardona.[7] In the present work, we use two well-known features in the Raman spectra of $YBa_2Cu_3O_{7-\delta}$ to monitor the oxygen concentration δ of the surface layer, as well as the oxygen order in O(1) and O(5) sites of a $YBa_2Cu_3O_7$ single crystal: (1) The intensity of a Raman-forbidden line in the range 580–600 cm^{-1} (subsequently referred to as the 580-cm^{-1} mode in this investigation) which appears in the spectra upon heating[8] or intense laser excitation,[9,10,11] and (2) The frequency of the 500-cm^{-1} O(4) z-axis vibration which depends strongly on δ.[5,6] The 580-cm^{-1} mode has been attributed to an infrared-active mode becoming allowed in Raman spectra by either (1) oxygen disorder in the Cu(1)-O(1) chains[9] or (2) anharmonic coupling between Raman and IR modes.[10,11] We attempt to identify the mode which is responsible for the 580-cm^{-1} feature in this investigation, and clearly establish that oxygen disorder (through diffusion) gives rise to part of the 580-cm^{-1} mode intensity.

We obtain Raman spectra by irradiating a sample of $YBa_2Cu_3O_7$ with laser radiation ($\lambda = 514$ mm from an Ar laser), and collecting the scattered light in the usual way. Laser energy is transformed into heat within the optical absorption length of the material, which for $YBa_2Cu_3O_7$ is ~ 0.06 μm or approximately 150 lattice spacings.[12] The temperature of the bulk of the sample during these experiments depends very much on the type of thermal mounting, and therefore we have taken care in these experiments to ensure good thermal contact with an aluminum heat sink. Since it is important to be able to estimate the temperature of the sample surface as a result of laser heating we have recorded the steady-state thermopower voltage between the surface and the heat sink of the sample. The difference of temperature between contacts of Au-$YBa_2Cu_3O_7$-Au was found to be in the range of 20 K for 10-mW incident laser power. Previous measurements of stokes/antistokes scattering intensity ratios show the heating of the surface with 10-mW excitation to be in the range 20–40 K, in agreement with the thermopower voltage measurements. We therefore treat laser powers below 10 mW as noninvasive from the point of view of the present investigation, whereas higher laser powers may rise the surface temperature (approximately linearly with laser power) to the point where oxygen outdiffusion takes place.

In Fig. 1 the Raman spectra are shown as a function of laser intensity and time. The laser was focused tightly onto a polished surface of the sample at room temperature in air and spectra recorded first with low intensity, 10 mW (~ 1 kW/cm^2), then with 250 mW (~ 25 kW/cm^2) and then in the same position after 10 min again with low-intensity laser light. In Fig. 1 we see that the position of the 500-cm^{-1} peak shifts to lower frequency by about 15 cm^{-1} upon exposure to high-intensity laser (middle trace), when compared to the spectrum obtained with low laser power (bottom trace). This frequency shift corresponds to reduction of oxygen concentration from $\delta \sim 0$ to $\delta \sim 0.8$.[5,6] Within 10 min however, we observe in the top trace of Fig. 1 an unambiguous increase in frequency of 5 ± 1 cm^{-1}, showing that oxygen has reen-

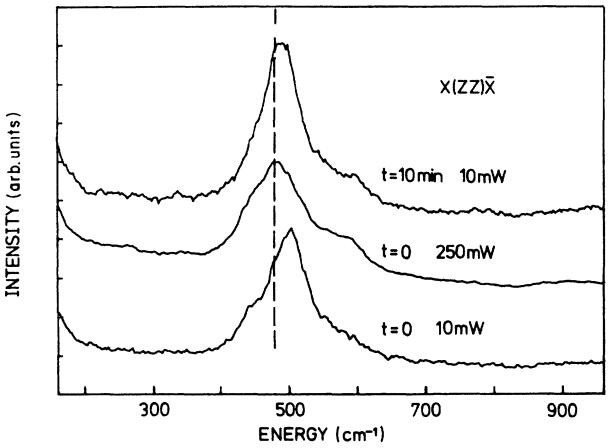

FIG. 1. Raman spectra of $YBa_2Cu_3O_7$ with different laser intensities and time intervals. The delayed spectrum (top) shows a visible shift towards higher frequency as a result of oxygen diffusion back into the surface. (Only data taken with low laser power can be used to determine oxygen concentration δ—see text.)

tered the surface and $\delta \sim 0.6$ after 10 min.

We plot the frequency of the 500-cm^{-1} phonon as a function of laser intensity in Fig. 2 of (a) the sample air and (b) the sample in vacuum. (The two paths shown may be viewed as heating and cooling cycles, with temperature along the abscissa.) The initial frequency of the 500-cm^{-1} mode in both cases corresponds to $\delta \sim 0$. As laser power is increased, we expect that above 380 °C oxygen will start to diffuse out of the surface.[3] The out-diffusion threshold clearly depends on the partial pressure of oxygen outside the sample, as is shown by the different behavior for the sample in vacuum and the sample in air. In vacuum the frequency of the 500-cm^{-1} line starts to drop at around 100 mW (~ 10 kW/cm^2), whereas we find that the frequency of the same line starts to drop above 150 mW (15 kW/cm^2) in air. The final (low intensity) positions of the 500-cm^{-1} peak in this experiment correspond to oxygen concentrations of (a) $\delta = 0.5 \pm 0.05$ for the sample in air (488 cm^{-1}) and (b) $\delta = 0.9 \pm 0.05$ for the sample in vacuum (480 cm^{-1}). (So far we have been using the published frequency shifts as a function of δ of Thomsen *et al.*[6]) We see that in both cases there is irreversible oxygen depletion in the surface layer of the material at high laser intensity as a result of raised surface temperature, but some oxygen is found to diffuse back into the scattering volume both in air and in vacuum upon removal of the heat source. In order to estimate the time of diffusion, we have recorded the frequency of the 500-cm^{-1} phonon with low-intensity excitation after 1 min and after 10 min. The result is shown in the last two points of the vacuum temperature cycle in Fig. 2. The 500-cm^{-1} peak shifts from 474 cm^{-1} to 481 cm^{-1} within 10 min. The subsequent shift with time (after 30 min) we have found to be small. We suggest that this is clear evidence that oxygen diffusion takes place from the bulk of the material back into the surface at room temperature with a diffusion time of the order of 10 min. This time we observe to be independent of the maximum laser power (and hence the amount of oxygen depleted) for laser powers above 100 mW. These results also show that the published shift of the 500-cm^{-1} phonon frequency with δ of Thomsen *et al.*,[6] and other workers[5] applies to equilibrium conditions, where δ is determined gravimetrically. The surface however, may have a different (higher) oxygen content due to shell formation,[3] and therefore the $\delta = 1$ position of this line is actually closer to 470 cm^{-1} than 480 cm^{-1}, as shown in Fig. 2 by the shift in frequency of the last point after 10 min.

Simultaneously with the shift in the 500-cm^{-1} phonon frequency with laser power and time in Fig. 1, we also observe in the spectra in Fig. 1 the shoulder at 580 cm^{-1} at high laser power (middle trace), which drops in intensity as the laser power is reduced (top trace). In Fig. 3 we plot the intensity of the 580-cm^{-1} shoulder as a function

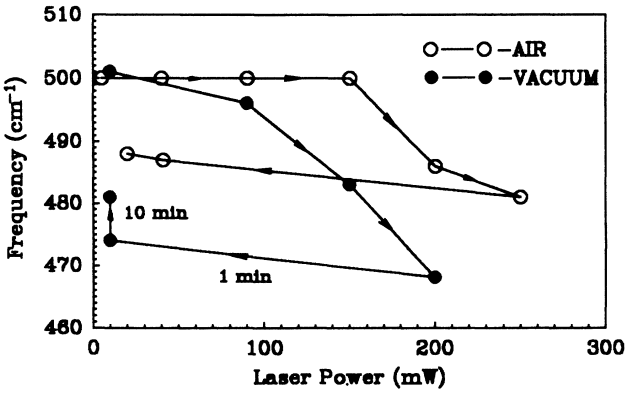

FIG. 2. Frequency of the 500-cm^{-1} O(4) z-axis vibration as a function of laser intensity for the sample in air and in vacuum. All data except the last point of the vacuum cycle were taken within approximately 1 min of each other.

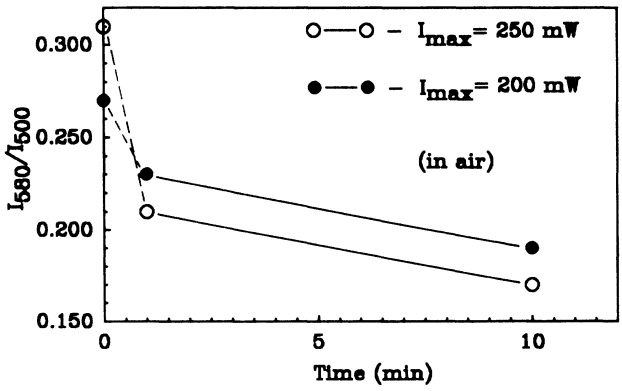

FIG. 3. Normalized intensity of the 580-cm^{-1} feature as a function of time. Open circles correspond to higher initial laser power (surface temperature) and result in $\delta \approx 0.9 (\omega_{final} = 481$ $cm^{-1})$. Solid circles correspond to lower initial laser power and $\delta \approx 0.6 (\omega_{final} = 487$ $cm^{-1})$. The greater intensity of the 580-cm^{-1} peak with higher oxygen concentration links the presence of oxygen in O(1) and O(5) sites with the 580-cm^{-1} feature.

of time after intense laser excitation at $t=0$. The intensity of the 580-cm^{-1} shoulder is obtained by first fitting the 500-cm^{-1} mode to a Lorentzian lineshape and then fitting the subtracted spectrum to another Lorentzian at 580 cm^{-1}. The two sets of measurements in Fig. 3 correspond to two different maximum laser excitation intensities (at $t=0$), and therefore different δ at $t=0$. We observe a fast drop in intensity within 1 min (dashed line) and a further smaller drop in 10 min (solid). This behavior clearly links the intensity of the 580-cm^{-1} feature with the frequency shift of the 500-cm^{-1} line. As oxygen diffuses from the bulk $YBa_2Cu_3O_7$ into the $YBa_2Cu_3O_6$ surface, it will do so by hopping via the O(1) and O(5) vacancy sites. In nonequilibrium conditions, its presence in O(5) sites will destroy long-range order and therefore we should expect to observe the otherwise forbidden 580-cm^{-1} infrared-active mode in Raman spectra. As equilibrium conditions as established, oxygens in the vacancy sites will tend to form some sort of long-range order,[2] most likely in domains of ordering in O(1) positions and domains of order in O(5) positions. (Such ordering corresponds to twinning in the orthorhombic $YBa_2Cu_3O_7$ structure.) The intensity of the 580-cm^{-1} line will therefore be reduced as ordering takes place. The very similar timescale of oxygen ordering (obtained from the 580-cm^{-1} line intensity) and diffusion (i.e., δ from the 500-cm^{-1} peak position) shows that indeed diffusion takes place via oxygen hopping along the vacant O(1) and O(5) chain sites. In Fig. 3 we observe that the final ($t=10$ min.) intensity of the 580-cm^{-1} mode is lower when the material is close to $\delta=1$ than when $\delta\approx 0.6$. This is consistent with the hypothesis above, since in $YBa_2Cu_3O_6$, i.e., $\delta=1$ material, no oxygen is present in the O(1) and O(5) sites.

The measurements above are all for diffusion along the orthorhombic *a* or *b* axes and therefore give the diffusion rate of oxygen along the O(1) and O(5) chain sites in tetragonal $YBa_2Cu_3O_6$. We have not been able to obtain data for oxygen transport along the crystal *c* axis, as the Raman intensities of the 500-cm^{-1} mode as well as the 580-cm^{-1} feature are much smaller than in the geometry used above. The necessarily longer accumulation times prevent us from looking at features in the spectra which vary with minute lifetimes.

We are not aware of any data on low-temperature diffusion in these materials. The activation energy of 0.4 eV for diffusion in $YBa_2Cu_3O_{7-\delta}$ with $\delta=0.38$ is consistent with the diffusion times that we observe in the oxygen-depleted surface. We cannot compare directly the results of our experiments with the diffusion rates of Tu *et al.*[3] however, since we must consider that the diffusion takes place in the presence of a potential gradient. By depleting oxygen from the surface layer, we create a gradual metal (bulk)-insulator (surface) junction, with an associated potential gradient. The effect of this potential should be fully taken into account in calculation of the diffusion rates for the case of diffusion into an oxygen depleted surface.

A possible objection to the interpretation of oxygen diffusion and hopping we have given above is that the sample as a whole is cooling during the 10 min period we are observing the changes in the Raman spectra, and that this is the cause of the observed features. This we can eliminate using the following considerations. We can set up a thermal diffusion problem to determine the surface temperature of our sample. We start with a steady-state temperature distribution and suddenly switch off the heat source. The solution to such a problem has been given by Carslaw and Jaeger.[13] The time for temperature to drop to half its maximum value is given approximately by $t_{1/2}=0.4l^2/\kappa$, where $\kappa=1.74\times10^{-6}$ m^2s^{-1}, is the thermal diffusivity of $YBa_2Cu_3O_7$ and $l=1$ mm is the sample thickness. If we take $l=3$ mm, to allow for the ~ 0.1 mm of glue (GE varnish) between the sample and the substrate, we obtain $t_{1/2}\sim 2$ s, in excellent agreement with a value of time constant of $t_{1/2}\sim 1.5$ s we have measured for the thermopower voltage drop between the surface and the substrate of the sample as the laser is switched off. Temperature can therefore be eliminated as the cause of the observed slowly changing features in the Raman spectra.

So far we have not considered the changes happening on a shorter timescale with $\tau<1$ s. In order to monitor Raman spectra on a shorter timescale, we have devised a time-resolved Raman measurement system shown in Fig. 4, whereby we can obtain Raman spectra at times limited by our detector gating capability or the laser pulse sequence. The pulse sequence which is shown in Fig. 4 is constructed by mounting neutral density (n.d.) filters on a chopper wheel. The ratio of intensities $I_{\text{pulse}}/I_{\text{probe}}$ of the probe pulses can be varied by the density of the n.d. filters. In our experiment we set the ratio of intensities so that we can assume that the heating of the subsequent probe laser pulses is negligible ($I_{\text{pulse}}\gg I_{\text{probe}}$). The detector, a gated microchannel-plate-intensified linear array detector is open during the delayed probe pulse at $t=t_0+\Delta t$ and closed at other times. Due to the chopper, we were limited in the present experiments to a time resolution of 1 ms.

In Fig. 5, we observe the Raman spectra of $YBa_2Cu_3O_7$ at various times after excitation. Little difference is ob-

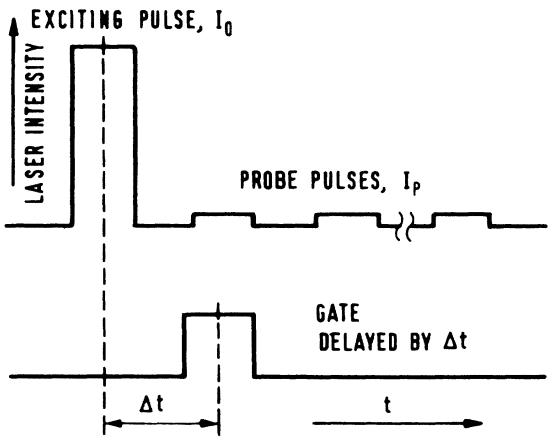

FIG. 4. The pulse sequence illustrating the time-resolved Raman measurements.

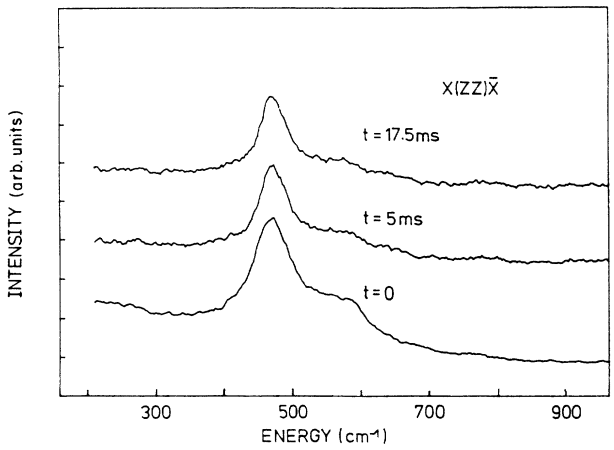

FIG. 5. Spectra of $YBa_2Cu_3O_7$ as a function of time.

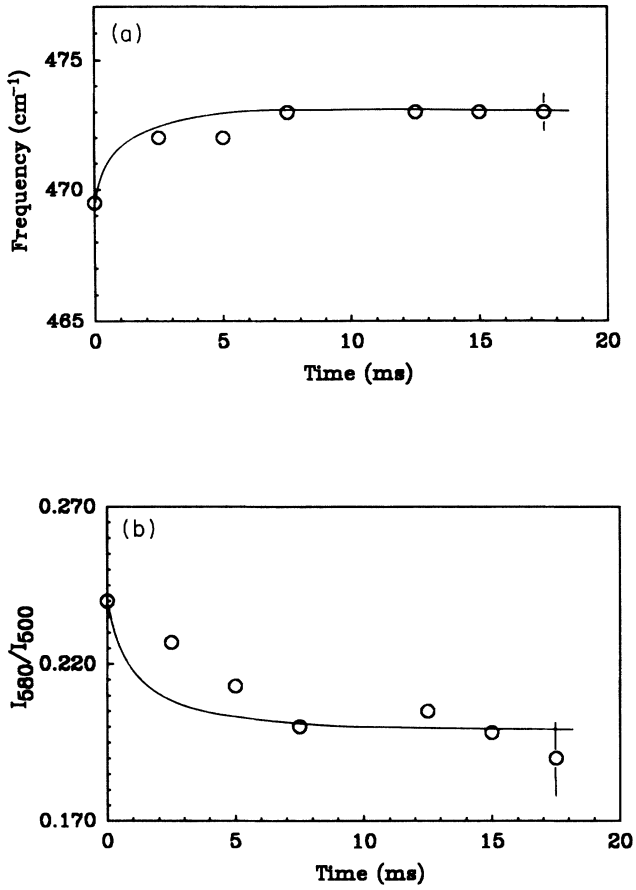

FIG. 6. (a) Frequency of the 50-cm^{-1} mode as a function of time. The solid line is the calculated temperature of the sample surface (see text). (b) Normalized intensity of the 580-cm^{-1} feature as a function of time. The solid line represents the scaled form of the temperature decay of the sample surface.

served between the delayed spectra at 5 and 17.5 ms, whereas the intensity of the 580-cm^{-1} mode clearly drops between $t=0$ and the delayed spectra. Similarly, the frequency of the 500-cm^{-1} mode also increases between the $t=0$ and the delayed spectra. The fitted 500-cm^{-1} mode frequency shift and normalized intensity of the 580-cm^{-1} peak are shown in Figs. 6(a) and 6(b) respectively. In both cases, there is a clear change in frequency (intensity) between the $t=0$ position compared to delayed spectra, and a small further change within ~2 ms. The thermal relaxation problem in this case is very different to the previous case and the raised temperature of the scattering volume due to laser heating needs to be taken into account. We use the surface heat generation model[14] to calculate the surface temperature as a function of time. The model consists the surface temperature of a thick slab heated on the surface by a short laser pulse. For the case where the absorption length, λ is much less than the dimension of the sample, the surface temperature is given by

$$\Delta T(z=0,t)=\frac{2I_{\text{pulse}}(1-R)}{K}\frac{\sqrt{\kappa t}}{\sqrt{\pi}}[\sqrt{(t/\tau)}-\sqrt{(t/\tau-1)}] \quad \text{for } t>\tau\,, \tag{1}$$

where R is the reflectivity, $\kappa=K/\rho c$ is the thermal diffusivity as before, ρ is the density, c is the specific heat, and τ is the pulse length. The maximum temperature of the sample surface is given by (1) with $t=\tau$. The model assumes a top-hat laser pulseshape which approximates well the shape of our chopped pulses. The solid lines in Fig. 6 are fitted to the temperature functional form (1) of the sample surface. In both cases, a scaling factor is the only fitting parameter. The other constants used in the calculation are given in Table I. Both the frequency shift and the intensity of the 580-cm^{-1} mode as a function of time are reasonably well described by the functional form of the temperature of the surface layer. The maximum value of surface temperature, $\Delta T=960$ K, calculated from (1) is much too high, however, and is well above melting temperature. The discrepancy arises because the uncertainty in the constants used for calculating ΔT at $t=\tau$ in (1). The functional form of the temperature decay however does not depend on the values of the constants, and we therefore conclude that within experimental accuracy both the frequency shift of the 500-cm^{-1} mode and the intensity of the 580-cm^{-1} feature follow the temperature of the scattering volume on the millisecond timescale.

Let us consider the origin of the temperature-dependent features. The simplest explanation for the appearance of the 580-cm^{-1} line in addition to the disorder-induced intensity is that of anharmonic coupling of the 500-cm^{-1} mode to other modes forbidden in Raman spectra by symmetry. As the amplitude of vibration of the atom involved increases, higher-order terms in the expansion of the vibrational energy with vibrational coor-

TABLE I. Constants used in calculating $\Delta T(0,t)$ (Eq. 1).

Thermal conductivity K (at 300 K)[a]	5 $W mol^{-1} K^{-1}$
Specific heat capacity c_p (at 300 K)[b]	300 $J mol^{-1} K^{-1}$
Density ρ	6.38 g/cm^3
Reflectivity R (at 300 K)	0.2
Pulse length τ	1 ms
Laser spot diameter	30 μm
Absorption length at 514.5 nm	0.06 μm

[a]Reference 18.
[b]Reference 19.

dinate become important. In particular, the potential for the vibration may include the coordinates of a neighboring atom or ion.[15] As a result, the coupled mode may also become visible in the Raman spectrum. In addition one may observe an anomalous frequency shift of the anharmonic mode with temperature as a consequence of the asymmetric vibrational potential of the anharmonic mode. As the amplitude of vibration increases, the center frequency of the mode shifts. In the case of the 500-cm^{-1} phonon, which has a large, nonlinear frequency shift with temperature[8,11] we observe an apparent decrease of intensity with increasing temperature, while the shoulder at 580 cm^{-1} increases in intensity. The most likely candidate for the 580-cm^{-1} shoulder is an infrared mode involving mainly the z-axis motion of O(1) and O(4) atoms together with small amplitude z-axis motion of Cu(1) and even smaller displacements of O(2) and O(3) atoms.[16] The frequency of this mode has been calculated[16,17] to be between 509 and 555 cm^{-1}, although it has so far not been observed in IR spectra in this frequency range. This may indicate that it is overdamped and therefore broad, especially as it involves O(1) atom motion. Other IR modes in this frequency range do not involve any motion of the O(4), Cu(1), or O(1) atoms, but involve rather for the most part the x (or y) motion of the O(2) [O(3)] atoms and are therefore less likely to be coupled to the 500-cm^{-1} Raman mode. The latter modes are strongly visible as sharp features in the region of 570-cm^{-1} in the IR spectra.

So far we have considered anharmonicity of the 500-cm^{-1} and/or 509-cm^{-1} IR modes as the cause of the temperature-dependent features, but we should also mention the possibility of fast tunneling of oxygen positions at high temperatures which may occur as a result of the anharmonic potentials of the modes involved. In such a case oxygen would tunnel between two positions, possibly vacant O(1) and O(5) sites or between a vacancy and an interstitial position. It is not possible at present to predict what effect that would have on the Raman spectra, but it certainly may be fast enough to account for the observed fast relaxation of both the 500-cm^{-1} phonon frequency and 580-cm^{-1} mode intensity on the millisecond timescale.

In summary, we observe oxygen diffusion at room temperature within the oxygen-depleted surface (<0.1 μm) of $YBa_2Cu_3O_7$ single crystals. We perform Raman measurements as a function of time after heating the surface and ejecting oxygen out of the material with a strong laser pulse. The diffusion is shown to proceed via hopping of oxygen in O(1) and O(5) sites. The oxygen out-diffusion, which appears to be a fast process is markedly different at room temperature in air when compared to vacuum and shows that the out-diffusion threshold depends on the oxygen partial pressure outside the sample. Time-resolved Raman spectra with millisecond resolution show fast relaxation of both the Raman-forbidden 580-cm^{-1} peak intensity and frequency shift of the O(4), z-axis, 500-cm^{-1} mode in Raman spectra. These features, which appear to follow closely the temperature of the surface are suggested to be due to the coupling of the 500-cm^{-1} apex O(4) vibration with an overdamped infrared mode involving chain O(1) and O(4) atoms. This may explain the high-temperature features observed in Raman spectra, as well as confirm that anharmonicity is an important feature of the high-T_c oxides, with special relevance to polarizability theories of high-T_c.

*Present address: Department of Physics, Institute for Polymers and Organic Solids, University of California, Santa Barbara, CA 93106.

[1]J. D. Jorgensen *et al.*, Phys. Rev. B **36**, 3608 (1987).
[2]M. A. Alario Franco, *Proceedings of the Conference on Oxygen Disorder Effects in High-T_c Superconductors, Trieste, 1989,* edited by J. L. Miran-Lopez and I. K. Schuller (Plenum, New York, 1990); also S. Amelinckx *et al., ibid.*
[3]K. N. Tu *et al.*, Phys. Rev. B **39**, 304 (1989).
[4]J. Karthikeyan *et al.*, Solid State Commun. **70**, 297 (1989).
[5]R. M. Macfarlane, H. J. Rosen, E. M. Engler, R. D. Jacowitz, and V. Y. Lee, Phys. Rev. B **38**, 284 (1988).
[6]C. Thomsen, R. Liu, A. Wittlin, L. Genzel, M. Cardona, E. Schönherr, W. Bauhofer, and W. König, Solid State Commun. **65**, 55 (1988).
[7]C. Thomsen and M. Cardona, in *Physical Properties of High-T_c Superconductors,* edited by D. M. Ginsberg (World Scientific, Singapore, in press).
[8]K. F. McCarty, J. C. Hamilton, R. N. Shelton, and D. S. Ginley, Phys. Rev. B **38**, 2914 (1988).
[9]V. N. Denisov, B. N. Marvin, V. B. Podobedov, I. V. Alexandrov, A. B. Bykov, A. F. Goncharov, and O. K. Mel'nikov, Phys. Lett. A **130**, 411 (1988).
[10]D. Mihailović and J. Šolmajer, in *High-T_c Superconductors:*

Electronic Structure, edited by A. Bianconi and A. Marcelli (Pergamon, Oxford, 1989).
[11]D. Mihailović and C. M. Foster, Solid State Commun. **74**, 753 (1990).
[12]J. Humlicek, M. Garriga, M. Cardona, B. Gegenheimer, and E. Schönherr, Solid State Commun. **60**, 1071 (1988).
[13]H. S. Carslaw and J. C. Jaeger, *Conduction of Heat in Solids* (Oxford University Press, New York, 1959).
[14]J. H. Bechtel, J. Appl. Phys. **46**, 1585 (1975).
[15]R. Cowley, in *The Raman Effect,* edited by A. Anderson (Dekker, New York, 1971).
[16]L. Genzel, A. Wittlin, M. Bauer, M. Cardona, E. Schlönherr, and A. Simon, Phys. Rev. B **40**, 2170 (1989).
[17]R. Liu, C. Thomsen, W. Kress, M. Cardona, B. Gegenheimer, F. W. deWetet, J. Prade, A. D. Kulkarni, and U. Schröder, Phys. Rev. B **37**, 7971 (1988).
[18]A. Jezowski *et al.*, Physica **153-155C**, 1347 (1988).
[19]T. Laegreid *et al.*, Physica **153-155C**, 1026 (1988).